

## On the Impact of Heterogeneous Chemistry on Ozone in the Tropopause Region

S.K. Meilinger<sup>1,2</sup>, B. Kärcher<sup>3</sup>, R. von Kuhlmann<sup>1</sup> and Th. Peter<sup>2</sup>

**Abstract.** We examine the impact of heterogeneous chemistry involving liquid aerosol and ice particles on net ozone ( $O_3$ ) production rates under conditions representative of the midlatitude upper troposphere (UT) and lowermost stratosphere (LS). We demonstrate that heterogeneous effects are controlled by nitrogen oxides ( $NO_x$ ) and by the location of the air masses relative to the tropopause (TP). The net effect of heterogeneous chemistry is to decrease net  $O_3$  production below the TP (via heterogeneous  $HO_2$  loss) and to cause  $O_3$  destruction above the TP (via heterogeneous chlorine (Cl) activation). In the UT, gas phase chemistry due to non-methane hydrocarbons (NMHCs) can become as important for  $O_3$  chemistry as heterogeneous reactions, and removal of  $HO_2$  by particles can become more important than changes of hydrogen oxides ( $HO_x$ ) through heterogeneous bromine (Br) chemistry. In the humid LS, Cl activation can become sufficiently large, so that  $O_3$  depletion occurs at all conceivable values of  $NO_x$ . Such cold and humid conditions occur frequently enough to reduce the average ozone production rates in the midlatitude LS by more than 10%.

### Introduction

Uncertainties in the role of  $NO_x$  ( $=NO+NO_2$ ) in controlling  $O_3$  chemistry lead to numerous research activities during the past decades. Most recently,  $NO_x$ - $O_3$  relationships were studied during major field campaigns [SONEX/POLINAT-2, 1999] and assessments on atmospheric impacts of aviation [IPCC, 1999]. Besides aviation, sources of  $NO_x$  in the TP region include surface pollution in conjunction with convective transport, lightning, and stratospheric injections. The effect of  $NO_x$  on  $O_3$  varies strongly with altitude. This is caused by strong gradients of chemical species involved in  $NO_x$ -catalyzed  $O_3$  chemistry.

We extend previous studies investigating the effect of  $NO_x$  on  $O_3$  [e.g., Ehhalt and Rohrer, 1995; Groöf et al., 1998] by considering halogen chemistry and heterogeneous reactions on liquid and ice particles, as both may affect  $NO_x$  and  $O_3$ . Heterogeneous chemistry exhibits a strong dependence on  $NO_x$  concentration as this influences the partitioning of the reacting species. Conversely, heterogeneous reactions influence  $NO_x$  through denoxification and halogen repartitioning.

As background  $NO_x$  concentrations at the TP vary by more than an order of magnitude [Brunner et al., 1998], it might be crucial to know the effect of  $NO_x$  changes for various background levels. Therefore, we systematically investigate the dependence of  $O_3$  on  $NO_x$  concentrations over a wide range of conditions, including heterogeneous chemistry.

### Photochemical Box Model

There is observational evidence and model indication that Cl activation on supercooled ternary  $H_2SO_4$ - $HNO_3$ - $H_2O$  solution (STS) droplets [Keim et al., 1996] and cirrus ice particles [Borrmann et al., 1996] might occur at the midlatitude TP. At temperatures well above the  $HNO_3$ -dew point  $T_{dew}$  (defined as the temperature below which the mass of liquid  $HNO_3$  exceeds that of  $H_2SO_4$ ), heterogeneous Br reactions are faster than the corresponding Cl reactions. Calculations suggest that heterogeneous Br chemistry converts  $H_2O$  into  $HO_x$  ( $=OH+HO_2$ ), and  $NO_x$  into  $HNO_3$ , leading to enhanced  $O_3$  destruction in the stratosphere [Lary et al., 1996]. Hendricks et al. [1999] predict a similar effect of Br for moderate  $NO_x$  concentrations in the TP region. At high  $[NO]/[O_3]$  ratios, however, heterogeneous Br chemistry might lead to additional  $O_3$  production as it increases  $HO_x$  [Hendricks et al., 2000]. Recently, Jaeglé et al. [2000] reported airborne field measurements showing evidence for heterogeneous chemistry of  $HO_2$  in the UT. Furthermore, several NMHC species, for example acetone and peroxyacetyl nitrate (PAN), have been shown to play an important role in controlling  $HO_x$  levels there [e.g. Wennberg et al., 1998].

To account for each of these processes, we extended the stationary box model of Groöf et al. [1998]. It now includes

**Table 1.** Heterogeneous reactions on liquid (l) and ice (i) particles. Uptake coefficients  $\gamma$  on ice recommended by DeMore et al. [1997]; those depending on temperature,  $HNO_3$  and  $H_2O$  (indicated by  $\star$ ) calculated according to Peter [1997];  $\gamma$ s for  $HO_2$  recommended by Jacob [2000].

No.	Heterogeneous Reaction	$\gamma_l$	$\gamma_i$
H1	$N_2O_5+H_2O \rightarrow 2 HNO_3$	0.1	0.01
H2	$N_2O_5+HCl \rightarrow ClNO_2+HNO_3$	-	0.03
H3	$2 HO_2 \rightarrow H_2O_2+2 O_2$	0.2	0.025
H4	$2 OH \rightarrow H_2O_2$	0.1	0.01
H5	$ClONO_2+H_2O \rightarrow HOCl + HNO_3$	$\star$	0.3
H6	$ClONO_2+HCl \rightarrow Cl_2 + HNO_3$	$\star$	0.3
H7	$ClONO_2+HBr \rightarrow BrCl + HNO_3$	-	0.3
H8	$HOCl + HCl \rightarrow Cl_2 + H_2O$	$\star$	0.3
H9	$HOCl + HBr \rightarrow BrCl + H_2O$	$\star$	0.3
H10	$BrONO_2+H_2O \rightarrow HOBr + HNO_3$	$\star$	0.3
H11	$BrONO_2+HCl \rightarrow BrCl + HNO_3$	-	0.3
H12	$HOBr + HCl \rightarrow BrCl + H_2O$	$\star$	0.3
H13	$HOBr + HBr \rightarrow Br_2 + H_2O$	$\star$	0.1

<sup>1</sup>MPI für Chemie, Mainz, Germany

<sup>2</sup>ETH Laboratorium für Atmosphärenphysik, Zürich, Switzerland

<sup>3</sup>DLR Institut für Physik der Atmosphäre, Wessling, Germany

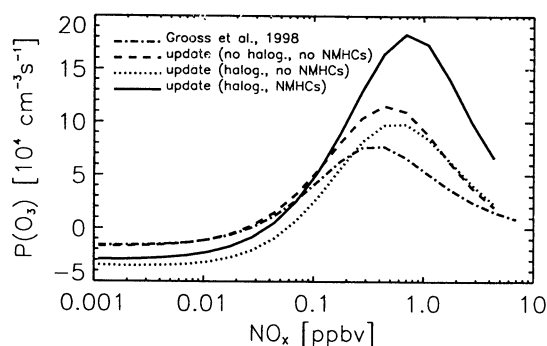
STS and cirrus ice particles, heterogeneous reaction cycles involving Cl and Br species, and heterogeneous reactions of HO<sub>2</sub> and OH (see Table 1). For gas phase reactions, we used updated kinetic reaction rates as recommended by *DeMore et al.* [1997] and *Atkinson et al.* [1999], including ethane, acetone, and their derivatives (with PAN), except for reactions of NO<sub>2</sub> and HNO<sub>3</sub> with OH, which were taken from *Sander et al.* [2000]. Photolysis rates were calculated with an update of the scheme by *Lary and Pyle* [1991], using the O<sub>3</sub> profile of the US standard atmosphere at 50°N and at a constant solar zenith angle of 60°.

The net O<sub>3</sub> production rate P(O<sub>3</sub>) (production minus destruction rates) is calculated as a snapshot after integrating the chemical equations over 2 hours to achieve photochemical equilibrium for short-lived species, using the numerical solver FACSIMILE. We discuss P(O<sub>3</sub>) as a function of initial NO<sub>x</sub> similar to *Grooß et al.* [1998]. The 2 hours integration time was used to allow comparability with *Grooß et al.* [1998], however in the case of heterogeneous Cl activation the model can be sensitive to this time scale as will be discussed later.

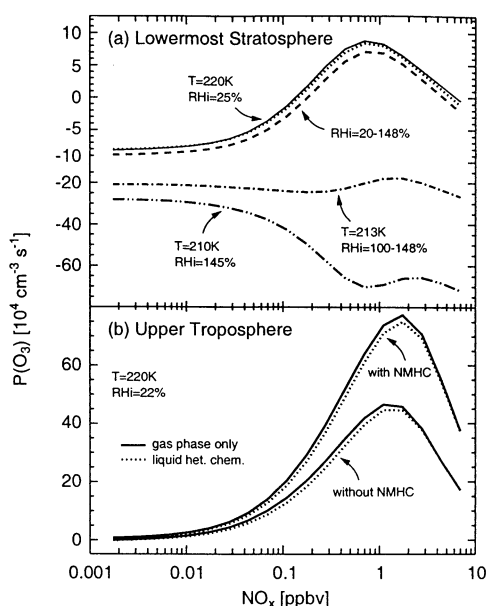
## Gas Phase Chemistry

Figure 1 shows P(O<sub>3</sub>) as a function of NO<sub>x</sub> mixing ratio as initialized by *Grooß et al.* [1998] (dash-dotted curve, see caption for details). We first compare with the updated model result for an atmosphere without NMHCs and halogens (dashed curve). The P(O<sub>3</sub>) maximum increases by about  $4 \times 10^4 \text{ cm}^{-3} \text{ s}^{-1}$  due to an increase in the HO<sub>x</sub> concentration resulting from improvements in the photolysis scheme [*Becker et al.*, 2000] (~75%) and from changes in the reaction rate coefficients (~25%).

Additional consideration of gas phase Br and Cl chemistry leads to a reduction of P(O<sub>3</sub>) (dotted curve). For low and medium NO<sub>x</sub> concentrations, the BrO/HO<sub>2</sub> catalytic cycle [*Lary*, 1996] efficiently destroys O<sub>3</sub>, increasing [NO]<sub>crit</sub> at which P(O<sub>3</sub>) equals zero. For high NO<sub>x</sub> concentrations,



**Figure 1.** Net O<sub>3</sub> production rates, P(O<sub>3</sub>) as calculated by *Grooß et al.* [1998] (dash-dotted curve), and with the present model using updated kinetic reaction rates (dashed curve) as a function of initial NO<sub>x</sub> mixing ratio in 2-hr simulations for 220 K and 200 hPa. Initialization according to *Grooß et al.* [1998], assuming 100 ppbv O<sub>3</sub>, 50 ppmv H<sub>2</sub>O, 60 ppbv CO, 0.2 ppbv HNO<sub>3</sub>, 30 pptv H<sub>2</sub>O<sub>2</sub>, 1.66 ppmv CH<sub>4</sub>, 0.5 ppmv H<sub>2</sub>. Dotted curve: addition of gas phase halogen chemistry assuming 80 pptv Cl<sub>y</sub> and 5.5 pptv Br<sub>y</sub>. Solid curve: addition of NMHC chemistry assuming 150 pptv acetone, 500 pptv ethane and 100 pptv PAN.



**Figure 2.** Calculations as for solid curve in Figure 1, but for different concentrations and including heterogeneous chemistry on background aerosol distinguishing between lowermost stratospheric (a) and upper tropospheric conditions (b). (a) Simulations for  $T$  and  $RH_i$  as indicated, with 100 pptv H<sub>2</sub>SO<sub>4</sub> condensed in background aerosol particles with number density  $500 \text{ cm}^{-3}$ . Solid curve: gas phase chemistry only. Dotted curve: including heterogeneous chemistry on background aerosol. Lower dash-dotted curve: including heterogeneous chemistry on STS particles ( $20 \mu\text{m}^2 \text{ cm}^{-3}$ ). Dashed and upper dash-dotted curves: including heterogeneous chemistry and averaging over  $RH_i$  as indicated. (b) Simulations at 220 K and  $RH_i = 22.5\%$  with and without NMHCs as indicated, with 200 pptv H<sub>2</sub>SO<sub>4</sub> in background aerosol particles with particle number density  $1000 \text{ cm}^{-3}$ . Solid curves: gas phase chemistry only. Dotted curves: including heterogeneous chemistry on background aerosol.

O<sub>3</sub> destruction due to the BrO/HO<sub>2</sub> cycle is hindered by the HO<sub>2</sub>+NO reaction competing with HO<sub>2</sub>+BrO. For the highest NO<sub>x</sub> levels shown, the formation of BrONO<sub>2</sub> via BrO+NO<sub>2</sub> leads to denoxification, shifting P(O<sub>3</sub>) to higher initial NO<sub>x</sub>. Finally, including NMHCs almost doubles the P(O<sub>3</sub>) maximum and reduces [NO]<sub>crit</sub> due to NMHC oxidation cycles and the related O<sub>3</sub> modifications (solid curve). For very high NO<sub>x</sub> levels, NMHCs are efficiently converted into the reservoir species PAN, limiting their O<sub>3</sub>-producing effect. At the same time the formation of PAN leads to denoxification, shifting the maximum of P(O<sub>3</sub>) to higher NO<sub>x</sub>.

## Heterogeneous Chemistry

**Liquid Aerosols.** Figure 2 shows the effect of background aerosols on P(O<sub>3</sub>) as a function of NO<sub>x</sub> for typical LS (a) and UT (b) conditions. The solid curves in Figure 2 show results for gas phase chemistry only, identical to the solid curve in Figure 1. However, as we here discuss two baseline cases separating UT and LS conditions, different mixing ratios of long-lived species are used to initialize the model (adopted from Table 2 of *Hendricks et al.* [1999]): 275 (29) ppbv O<sub>3</sub>, 44 (57) ppbv CO, 0.87 (0.17) ppbv HNO<sub>3</sub>, 75 (204) pptv H<sub>2</sub>O<sub>2</sub>, 1.7 ppmv CH<sub>4</sub>, 325 (145) pptv Cl<sub>y</sub> and 2.78 (0.98)

pptv  $\text{Br}_y$ , above (below) the TP. The NMHC mixing ratios were taken from *Singh et al.* [1997], assuming 100 pptv (1 ppbv)  $\text{C}_2\text{H}_6$ , 100 pptv (600 pptv) acetone and 40 pptv (150 pptv) PAN. We consider background  $\text{H}_2\text{O}$ - $\text{H}_2\text{SO}_4$  aerosols at  $T = 220$  K, and STS droplets at cold conditions of  $\sim 210$  K above the TP [*Gierens et al.*, 1999].

Due to the differences in  $\text{O}_3$ , CO, NMHCs, and  $\text{H}_2\text{O}$  concentrations,  $\text{P}(\text{O}_3)$  is generally higher below than above the TP. NMHCs, transported from the surface to the TP via convection, are more abundant below than above the TP. Consequently, we find the effect of NMHCs to be negligible in the LS (not shown in Figure 2a), while it may become important in the UT, as indicated by the difference between the two solid curves in Figure 2b. This highlights the importance to separate the two atmospheric regimes.

**Lowermost Stratosphere.** The dotted curve in Figure 2a shows  $\text{P}(\text{O}_3)$  including heterogeneous chemistry on background  $\text{H}_2\text{SO}_4$ - $\text{H}_2\text{O}$  aerosol at a typical temperature and relative humidity over ice ( $\text{RH}_i$ ) of 220 K and 25%, respectively [*Gierens et al.*, 1999]. In this case the aerosol effect on  $\text{P}(\text{O}_3)$  is very small. Heterogeneous chemistry becomes more important under ice supersaturated conditions, where  $\text{ClONO}_2 + \text{HCl}$  (H6 in Table 1) is the most efficient heterogeneous reaction. As temperatures approach  $T_{\text{dew}} = 209.4$  K, activation via  $\text{ClONO}_2 + \text{HCl}$  increases dramatically, leading to net  $\text{O}_3$  destruction in the entire  $\text{NO}_x$  regime (lower dash-dotted curve,  $T = 210$  K). This is due to the increasing solubility of HCl (and  $\text{HNO}_3$ ), enabling heterogeneous activation of up to 40 pptv of ClO, leading to ozone destruction rates of several  $10^5 \text{cm}^{-3} \text{s}^{-1}$ . The upper dash-dotted curve in Figure 2a shows the average effect of heterogeneous chemistry under ice supersaturated conditions derived from the distribution law for  $\text{RH}_i$  based on the MOZAIC data set. We averaged over  $\text{RH}_i = 100$ –148% using  $T = 213$  K as typical for the ice supersaturated LS [*Klaus Gierens*, priv. communication, 2000]. In the MOZAIC data set, ice supersaturation occurs in about 2% of the cases, which appears to be a small occurrence frequency. However, due to their large impact on ozone, these cases account for an average decrease of  $\text{P}(\text{O}_3)$  of  $\sim 10\%$  as shown by the dashed curve in Figure 2a (now averaged over sub- and supersaturated regions,  $\text{RH}_i = 20$ –148%). It is important to note that the degree of heterogeneous Cl activation does not only depend on  $T$  and  $\text{RH}_i$ , but also on the persistence of the supersaturation. As constant atmospheric conditions cannot be assumed for an arbitrarily long time period, we assumed this persistence to be the 2 hour integration time. Our model indicates that Cl activation increases if the STS particles persist longer than 2 hours, leading to even stronger ozone depletion.

**Upper Troposphere.** The dotted (solid) curves in Figure 2b show  $\text{P}(\text{O}_3)$  with (without) heterogeneous chemistry on background aerosol at typically 220 K and  $\text{RH}_i = 22\%$  [*Gierens et al.*, 1999] with and without NMHCs, as indicated. Independent of the presence of NMHCs, heterogeneous chemistry lowers the  $\text{P}(\text{O}_3)$  maximum by  $\sim 3\%$ . An analysis of the reaction rates shows that heterogeneous removal of  $\text{HO}_2$  (reaction H3) dominates over changes of  $\text{HO}_x$  through heterogeneous Br chemistry. Heterogeneous loss of  $\text{HO}_2$  – leading to slower photochemical production of  $\text{O}_3$  – is limited for high  $\text{NO}_x$  by the  $\text{HO}_2$  concentration it-

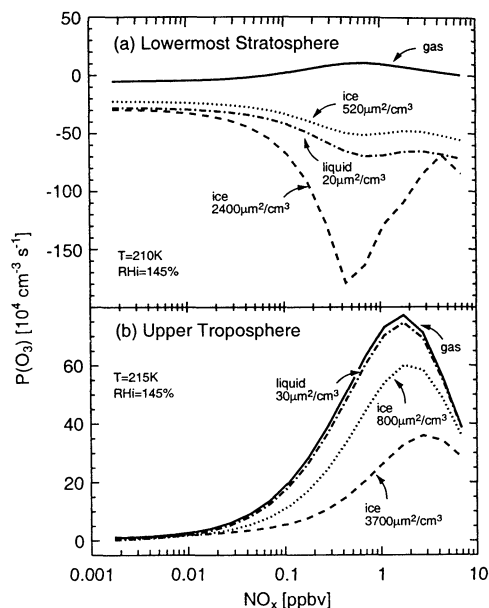


**Figure 3.** As in Figure 2, but for different  $T$  and  $\text{RH}_i$  and additionally including heterogeneous chemistry on ice particles. Solid curves: gas phase chemistry only. Dash-dotted curves: dilute droplets (a:  $500 \text{cm}^{-3}$ ; b:  $1000 \text{cm}^{-3}$ ). Dotted curves: low density cirrus cloud ( $0.1 \text{cm}^{-3}$ ). Dashed curves: high density cirrus cloud ( $10 \text{cm}^{-3}$ ).

self ( $\text{HO}_2 + \text{NO} \rightarrow \text{OH} + \text{NO}_2$ ). Heterogeneous  $\text{HO}_x$  destruction slightly increases  $[\text{NO}]_{\text{crit}}$ .

**Ice Particles.** Below the tropopause supersaturations with respect to ice may lead to the formation of cirrus clouds. In addition, we investigate the case that the observed stratospheric supersaturations lead to the formation of ice particles, although to date there is only limited observational evidence for the existence of ice particles above the TP [e.g., *Lelieveld et al.*, 1999; *Kärcher and Solomon*, 1999]. Figure 3 shows  $\text{P}(\text{O}_3)$  as a function of initial  $\text{NO}_x$  for typical LS (a) and UT (b) conditions. The solid curves show results from pure gas phase simulations. We compare the chemical effects of cirrus ice particles (dashed and dotted curves) with those of dilute droplets (dash-dotted curves).

**Lowermost Stratosphere.** Above the TP, ice formation leads to strong Cl activation ( $[\text{ClO}] = 35$ –190 pptv) and thus to  $\text{O}_3$  loss rates (Figure 3a) ranging from values comparable to STS (dash-dotted) at low ice surface areas (dotted) to more than twice as high at high surface areas (dashed). Again, the degree of Cl activation depends not only on surface area, but also on the cloud lifetime. Cl is mainly activated from  $\text{ClONO}_2$  (via H6). In the high cirrus surface area case (dashed curve) a deep minimum in  $\text{P}(\text{O}_3)$  develops, followed by a maximum at very high initial  $\text{NO}_x$  levels. A reaction rate analysis reveals that at low  $\text{NO}_x$  ( $< 0.4$  ppbv), the leading reaction sequence is  $\text{ClO} + \text{NO}_2 \rightarrow \text{ClONO}_2$  and  $\text{ClONO}_2 + \text{H}_2\text{O} \rightarrow \text{HOCl} + \text{HNO}_3$  followed by  $\text{HOCl} + \text{HCl} + h\nu \rightarrow 2\text{ClO} + \text{H}_2\text{O} + 2\text{O}_2$  (net), which also leads to substantial denoxification ( $\sim 0.3$  and  $2.5$  ppbv at the minimum and relative maximum of the dashed curve, respectively). At higher  $\text{NO}_x$  ( $> 0.4$  ppbv) HCl is used up and the produced HOCl photolyses to Cl and OH, which leads at the

same time to O<sub>3</sub> depletion (via Cl+O<sub>3</sub>) and O<sub>3</sub> production (via CH<sub>4</sub>+OH). For very high NO<sub>x</sub> (> 4 ppbv), this is limited by dehydrochlorination through production of HNO<sub>3</sub> and HNO<sub>4</sub> (via NO<sub>2</sub>+HO<sub>x</sub>). In contrast to the case with liquid aerosols (Figure 2a), we did not try to calculate average effects for ice clouds (the MOZAIC data do not apply to cloudy cases), but it is conceivable that at least as large effects as for liquid particles can be expected.

**Upper Troposphere.** Figure 3b shows that heterogeneous chemistry on ice decreases P(O<sub>3</sub>) below the TP. Similar to heterogeneous chemistry on liquid aerosol particles, the most important heterogeneous daytime effect on P(O<sub>3</sub>) is the heterogeneous loss of HO<sub>2</sub> (H3). This effect increases with increasing particle surface area, reducing HO<sub>2</sub> by a factor of 5 (2.5) in the high (low) surface case (compare the dotted and dashed curves in Figure 3b). As heterogeneous HO<sub>2</sub> loss is limited towards high NO<sub>x</sub> by abundance of HO<sub>2</sub>, the P(O<sub>3</sub>) maxima are shifted towards higher NO<sub>x</sub> mixing ratios. This shift increases with increasing surface area.

## Summary and Outlook

Our study reveals that the response of P(O<sub>3</sub>) on increasing NO<sub>x</sub> is influenced by halogens and NMHCs and can be significantly modified by heterogeneous reactions on ice and STS particles, while the effect of background aerosol is negligible. Besides NO<sub>x</sub>, we identified the origin of air masses (stratospheric or tropospheric) as a crucial factor determining the effectiveness of heterogeneous chemistry. Assuming constant atmospheric conditions over a period of 2 hours, we found the highest O<sub>3</sub> loss rates due to heterogeneous Cl activation in the presence of ice and STS particles above the TP.

Halogens, NMHCs, aerosols, and subvisible cirrus exhibit pronounced seasonal and regional variations around the mid-latitude TP. While progress has been achieved in better quantifying NO<sub>x</sub> emissions from aviation, at least over the North Atlantic, the abundances of organic species and their reactions with halogens are still poorly constrained by in situ and laboratory measurements. This study illustrates the need for reliable humidity and temperature statistics in the tropopause region. We further propose to include the effects of variable STS and cirrus cloud lifetimes in future chemical simulations, using realistic atmospheric trajectories. We found significant sensitivities of the calculated ozone net production rates on this parameter. Further research on the occurrence frequency, persistence time, and altitude of ice clouds is necessary to apply our results to a global scale.

**Acknowledgments.** We thank John Crowley, Johannes Hendricks and Andreas Meier for helpful discussions and Klaus Gierens for information on the MOZAIC humidity statistics. This work was partly supported by the Umweltbundesamt (Berlin), contract 104 02 814.

## References

Atkinson R. *et al.*, Summary of evaluated kinetic and photochemical data for atmospheric chemistry: Web Version 01/1999.  
 Becker, G. *et al.*, Stratospheric photolysis frequencies: Impact of an improved numerical solution of the radiative transfer equation *J. Atmos. Chem.*, 00, 1–13, 2000.

Borrmann, S. *et al.*, The potential of cirrus clouds for heterogeneous chlorine activation, *Geophys. Res. Lett.*, 23, 2133–2136, 1996.  
 Brunner D. *et al.*, Large-scale nitrogen oxide plumes in the tropopause region and implications for ozone, *Science*, 282, 1305–1309, 1998.  
 DeMore, W.B. *et al.*, Chemical kinetics and photochemical data for use in stratospheric modeling, Evaluation Number 12, *JPL Publication 97-4*, 269 pp., Pasadena, CA, 1997.  
 Ehhalt D.H., and F. Rohrer, The impact of commercial aircraft on tropospheric ozone, in: Bandy, A.R. (Ed.), *The chemistry of the atmosphere*, Royal Society of Chemistry, Cambridge, UK, 105–120, 1995.  
 Gierens, K. *et al.*, A distribution law for relative humidity in the UT and LS derived from three years of MOZAIC measurements, *Ann. Geophysicae*, 17, 1218–1226, 1999.  
 Grooß, J.-U. *et al.*, Impact of aircraft emissions on tropospheric and stratospheric ozone. Part I: Chemistry and 2D-model results, *Atmos. Environ.*, 32, 3173–3184, 1998.  
 Hendricks J. *et al.*, Heterogeneous reactions on and in sulfate aerosols: Implications for the chemistry of the midlatitude tropopause region, *J. Geophys. Res.*, 104, 5531–5550, 1999.  
 Hendricks J. *et al.*, Implications of subsonic aircraft NO<sub>x</sub> emissions for the chemistry of the LS: Model studies on the role of bromine, *J. Geophys. Res.*, 105, 6745–6759, 2000.  
 Intergovernmental Panel on Climate Change (IPCC), Aviation and the Global Atmosphere, J.E. Penner *et al.* (Eds.), Cambridge Univ. Press, 1999.  
 Jacob, D.J., Heterogeneous chemistry and tropospheric ozone, *Atmos. Environ.*, 34, 2131–2159, 2000.  
 Jaeglé, L. *et al.*, Photochemistry of HO<sub>x</sub> in the UT at northern mid-latitudes, *J. Geophys. Res.*, 105, 3877–3892, 2000.  
 Kärcher, B. and S. Solomon, On the composition and optical extinction of particles in the tropopause region, *J. Geophys. Res.*, 104, 27441–27459, 1999.  
 Keim, E.R. *et al.*, Observations of large reductions in the NO/NO<sub>y</sub> ratio near the mid-latitude tropopause and the role of heterogeneous chemistry *Geophys. Res. Lett.*, 23, 3223–3226, 1996.  
 Lary D.J. and J.A. Pyle, Diffusive radiation, twilight and photochemistry, *J. Atmos. Chem.*, 13, 373–406, 1991.  
 Lary D.J. *et al.*, Heterogeneous atmospheric bromine chemistry, *J. Geophys. Res.*, 101, 1489–1504, 1996.  
 Lary D.J., Gas phase atmospheric bromine photochemistry, *J. Geophys. Res.*, 101, 1505–1516, 1996.  
 Lelieveld J. *et al.*, Chlorine activation and ozone destruction in the northern LS, *J. Geophys. Res.*, 104, 8201–8213, 1999.  
 Peter, Th., Microphysics and heterogeneous chemistry of polar stratospheric clouds, *Annu. Rev. Phys. Chem.*, 48, 785–822, 1997.  
 Sander S.P. *et al.*, Chemical kinetics and photochemical data for use in stratospheric modeling, Evaluation Number 13, *JPL Publication 00-3*, 74 pp., Web version 03/2000.  
 Singh, H.B. *et al.*, Trace chemical measurements from the northern midlatitude LS in early spring: Distributions, correlations and fate, *Geophys. Res. Lett.*, 24, 127–130, 1997.  
 SONEX/POLINAT-2, Airborne Missions, Special Section in *Geophys. Res. Lett.*, 26, 3053–3081, 1999.  
 Wennberg, P.O. *et al.*, Hydrogen radicals, nitrogen radicals and the production of O<sub>3</sub> in the upper troposphere, *Science*, 279, 49–53, 1998.

B. Kärcher, DLR Institut für Physik der Atmosphäre, D-82234 Weßling. R. von Kuhlmann and S.K. Meilinger, MPI Chemie, Postfach 3060, D-55020 Mainz. Th. Peter, ETH Atmospheric Sciences, Höggerberg HPP, CH-8093 Zürich. (smeili@mpch-mainz.mpg.de)

(Received March 31, 2000; revised November 6, 2000; accepted November 20, 2000.)